

# Local structural study of commercial grade $\text{M}\text{Ba}_2\text{Cu}_3\text{O}_{7-x}$ ( $\text{M} = \text{Y}$ and/or $\text{Gd}$ ) coated conductors by polarized Raman spectroscopy

Hankyoul Moon, Hae-Young Shin, Hye-Jin Jin, William Jo, and Seokhyun Yoon\*

*Department of physics, Ewha Womans University, Seoul, 03760, Korea*

(Received 16 November 2015; revised or reviewed 16 December 2015; accepted 17 December 2015)

## Abstract

In 1987, M. K. Wu and Paul Chu discovered  $\text{Y}_{1.2}\text{Ba}_{0.8}\text{CuO}_4$  (YBCO) with critical temperature ( $T_c$ ) of 93 K. It has significantly lowered the cost of cooling of a material up to the point where superconductivity set in. Utilizing the cost reduction of attaining superconductivity and the vast amount of research to understand characteristics of high temperature oxide superconducting materials, there has been effort to use a high temperature superconductor as a coated conductor. It is important to characterize the materials precisely for stable performance before commercializing. We used polarized Raman scattering spectroscopy to study structural and stoichiometric information regarding  $\text{YBa}_2\text{Cu}_3\text{O}_{7-x}$ ,  $\text{GdYBa}_2\text{Cu}_3\text{O}_{7-x}$ , and  $\text{GdBa}_2\text{Cu}_3\text{O}_{7-x}$  produced by three leading groups of producing commercial grade high temperature superconductor coated conductors American Superconductor Corporation, Superpower, and SuNAM.

*Keywords: Commercial-grade Coated Conductors, Polarized Raman spectroscopy, Microstructure*

## 1. INTRODUCTION

In 1986, J. Georg Bednorz and K. Alex Müller synthesized barium-doped compound of lanthanum and copper oxide with critical temperature of 35 K [1]. It was the first high critical temperature ( $T_c$ ) superconductor (HTS) found in ceramic materials. After that discovery, many researchers having been tried to find superconductors with higher  $T_c$ , and now HTS of mercury barium calcium copper oxide ( $\text{HgBa}_2\text{Ca}_2\text{Cu}_3\text{O}_8$ ) with critical temperature as high as 133 K have been synthesized [2, 3]. The first superconductor which has higher  $T_c$  than the boiling point of liquid nitrogen (77 K) is  $\text{YBa}_2\text{Cu}_3\text{O}_{7-x}$ . In this compound,  $T_c$  is maximized near 93 K around  $x = 0.15$  with the orthorhombic structure. However, superconductivity disappears in  $\text{YBa}_2\text{Cu}_3\text{O}_{7-x}$  around  $x = 0.6$  with tetragonal structure [4]. From 2000s, studies of rare earth materials such as gadolinium (Gd), samarium (Sm) replacing yttrium (Y) have been performed in many research groups and companies.

Coated conductors (CCs) have good characteristics for using in application to cables, generators and transformers [5, 6]. Recently, companies have been developing optimized methods to make coated conductors using HTS [7]. Among them, American Superconductor Corporation (AMSC), Superpower and SuNAM are leading the development of coated conductors. CCs are fabricated with metal organic chemical vapor deposition [8, 9], metal-organic deposition [10, 11] and/or co-evaporation [12, 13] in these companies. But each of CCs shows different characteristics such as performance, cost, and production rates because of the materials in superconducting

layer and buffer layers are all different company by company.

In this study, we studied local structural properties by polarized micro-Raman measurement about three commercial-grade CCs produced by AMSC, Superpower, SuNAM. In addition to the structural information that can be obtained, e.g., by XRD, polarized micro-Raman scattering measurements can provide information such as distribution of second phase in the surface and the orientation of grains in micrometer scale.

## 2. EXPERIMENTS

Three sets of coated conductor samples were prepared for this study: The first sample is  $\text{YBa}_2\text{Cu}_3\text{O}_{7-x}$  (YBCO) made by AMSC. This sample was fabricated by metal organic deposition (MOD) and the structure of this sample is Ag (1  $\mu\text{m}$ ) / YBCO (1  $\mu\text{m}$ ) /  $\text{CeO}_2$  (75 nm) / YSZ (75 nm) /  $\text{Y}_2\text{O}_3$  (75 nm) / metal alloy substrate (50 – 75  $\mu\text{m}$ ). Buffer layers are fabricated by solution-based processing [14]. The second one is  $(\text{Gd},\text{Y})\text{Ba}_2\text{Cu}_3\text{O}_{7-x}$  (GdYBCO) made by Superpower. This sample was fabricated by metal organic chemical vapor deposition (MOCVD) and the structure of this sample is Cu stabilizer (20  $\mu\text{m}$ ) / Ag (2  $\mu\text{m}$ ) / GdYBCO (1  $\mu\text{m}$ ) / buffer stack (1  $\mu\text{m}$ ) / substrate (50  $\mu\text{m}$ ) [15]. The third one is  $\text{GdBa}_2\text{Cu}_3\text{O}_{7-x}$  (GdBCO) made by SuNAM. This sample was fabricated by reactive co-evaporation by deposition and reaction (RCE-DR) and the structure of this sample is Ag (1  $\mu\text{m}$ ) / GdBCO (1.5  $\mu\text{m}$ ) /  $\text{LaMnO}_3$  (20 nm) /  $\text{MgO}$  (60 nm) /  $\text{Y}_2\text{O}_3$  (7 nm) /  $\text{Al}_2\text{O}_3$  (50 nm) / Hastelloy [16]. The details of the fabrication method of each sample are shown in [17-19].

To measure the three sets of samples, polarized

\* Corresponding author: syoon@ewha.ac.kr

Micro-Raman measurements were performed. Samples were excited with 10 mW of 488 nm (2.54 eV) diode laser focused to 1  $\mu\text{m}$  diameter spots using 100x microscope objective. For polarization measurement, the spectra were obtained with the incident and scattered light polarized in the following configurations in order to identify the symmetries of the phonon modes studied:  $(E_i, E_s) = (X, X)$ ,  $(E_i, E_s) = (X', X')$ ,  $(E_i, E_s) = (X, Y)$ ,  $(E_i, E_s) = (X', Y')$ , where  $E_i$  and  $E_s$  are the incident and scattered electric-field polarizations, respectively,  $X$ ,  $Y$ ,  $X'$ ,  $Y'$  are the  $[100]$ ,  $[010]$ ,  $[110]$ , and  $[1\bar{1}0]$  crystal directions, respectively. In our polarized Raman measurements, the angle between the polarization of the incident light and a nanowire was changed by rotating the incident polarization. When the polarization of the scattered light is parallel (perpendicular) to that of the incident light, we name that configuration parallel (perpendicular) polarized Raman measurement.

### 3. RESULT AND DISCUSSION

The crystal structure of  $\text{MBA}_2\text{Cu}_3\text{O}_7$  (MBCO) is shown in Fig. 1. In this figure, only the middle atom in the unit cell, denoted by  $M$ , is different between YBCO ( $M=\text{Y}$ ) and GdBCO ( $M=\text{Gd}$ ). These materials can have either orthorhombic or tetragonal phase, and superconducting properties are only observed in orthorhombic phase. The SEM images of each coated conductor are shown in Fig. 2. YBCO (a) has small grain size compare to GdYBCO (b) and GdBCO (c). As shown in Fig. 2, GdYBCO and GdBCO have some irregular pattern and this pattern shows different color in optical microscope (Figs. 4 (c) to (f)).

Unpolarized Raman spectra are shown in Fig. 3. In this figure, there are 5 peaks ( $140\text{ cm}^{-1}$ ,  $210\text{ cm}^{-1}$ ,  $333\text{ cm}^{-1}$ ,  $448\text{ cm}^{-1}$ ,  $494\text{ cm}^{-1}$ ) seen in YBCO, there are 6 peaks ( $143\text{ cm}^{-1}$ ,  $294\text{ cm}^{-1}$ ,  $335\text{ cm}^{-1}$ ,  $400\text{ cm}^{-1}$ ,  $500\text{ cm}^{-1}$ ,  $630\text{ cm}^{-1}$ ) observed in GdYBCO and the spectrum of GdBCO shows 6 peaks ( $143\text{ cm}^{-1}$ ,  $295\text{ cm}^{-1}$ ,  $326\text{ cm}^{-1}$ ,  $344\text{ cm}^{-1}$ ,  $502\text{ cm}^{-1}$ ,  $631\text{ cm}^{-1}$ ). It is well-known that  $140\text{ cm}^{-1}$  (YBCO) and  $143\text{ cm}^{-1}$  (GdYBCO) peaks are  $A_g$  mode induced by Cu-Cu stretching motion,  $210\text{ cm}^{-1}$  of YBCO is related to the oxygen disorder at the  $\text{Cu}(1)\text{-O}(4)$ - chains and  $448\text{ cm}^{-1}$  of

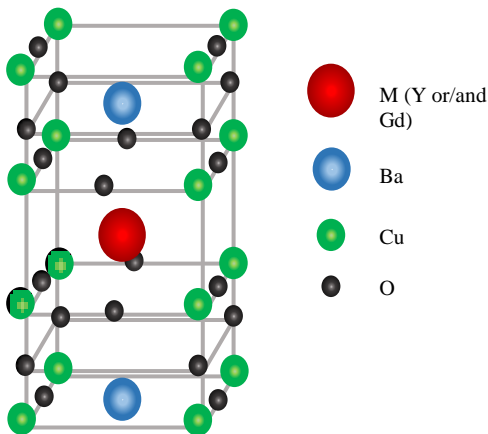


Fig. 1. Crystal structure of orthorhombic phase MBCO.

YBCO and  $400\text{ cm}^{-1}$  of GdYBCO are mainly due to in-phase  $z$ -displacements of the  $\text{O}(2)$  and  $\text{O}(3)$  oxygen atoms ( $A_g$  mode), respectively [20].  $294\text{ cm}^{-1}$  of GdYBCO and  $295\text{ cm}^{-1}$  of GdBCO came from second phase of  $\text{CuO}$  [21]. Main peaks that are not related to either disorder or second phases of MBCO ( $M = \text{Y}$  and/or  $\text{Gd}$ ) exist around  $330\text{ cm}^{-1}$  and  $500\text{ cm}^{-1}$ .  $333\text{ cm}^{-1}$  of YBCO,  $335\text{ cm}^{-1}$  of GdYBCO and  $326\text{ cm}^{-1}$  of GdBCO are associated with the same out-of-phase  $A_g$  mode in the  $\text{CuO}_2$  plane ( $\text{O}(2)+\text{O}(3)$ ) [22].

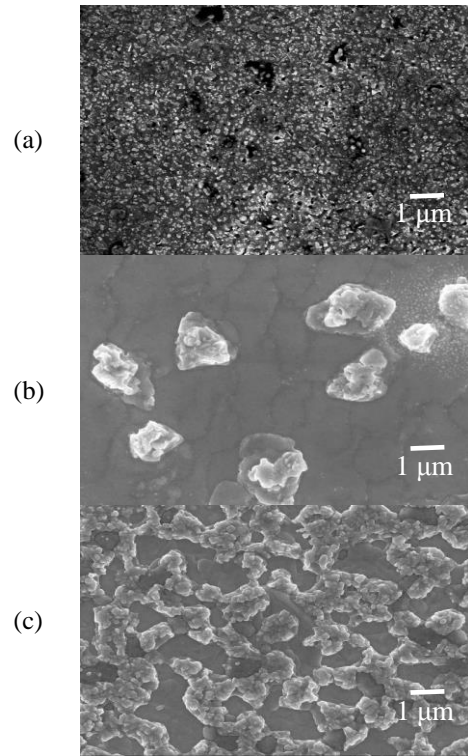


Fig. 2. SEM images of YBCO (a), GdYBCO (b) and GdBCO (c).

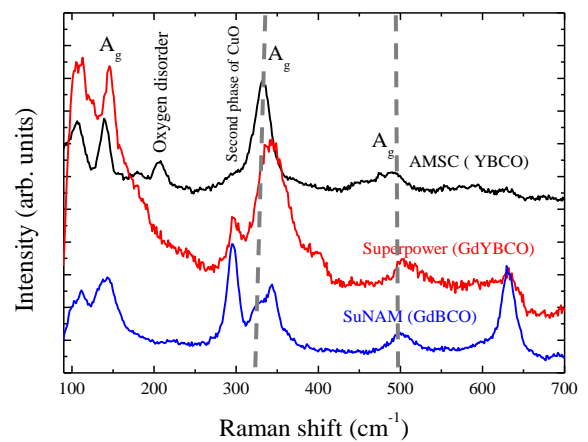


Fig. 3. Unpolarized Raman spectra of each CC. The spectra are offset for clarity. Dashed lines denote the frequencies of the  $\text{O}(2)+\text{O}(3)$  mode (around  $330\text{ cm}^{-1}$ ) and the apical oxygen ( $A_g$ ) mode (around  $500\text{ cm}^{-1}$ ).

In the case of pure orthorhombic structure the O(2)+O(3) mode should have  $A_g$  symmetry, but in the oxygen undepleted YBCO, the mode behaves like a  $B_{1g}$  mode [20]. Because a phonon mode frequency depends on the mass of the vibrating atom, difference in atomic mass of Y (88.906 g/cc) and Gd (157.25 g/cc) is to be seen as the relative peak positions in Raman spectra. In Raman measurements, a peak of GdBCO has lower frequency than that of YBCO because Gd is heavier than Y.  $494\text{ cm}^{-1}$  of YBCO,  $500\text{ cm}^{-1}$  of GdYBCO,  $502\text{ cm}^{-1}$  of GdBCO are  $A_g$  modes due to apical O(4). This mode is related to the oxygen contents and the vibration is along the  $c$ -axis. This mode tends to shift toward lower frequency when oxygen is insufficient and also largely reflects the structural disorder. From these two main modes, we can figure out the structural orientation of the samples. These samples can be grown into either the  $a$ -axis or the  $c$ -axis orientation. According to the Raman selection rule the  $a$ -axis oriented grains should not show O(2)+O(3) peak [23]. However, we clearly observed the O(2)+O(3) mode in all of the three samples so it is apparent that our samples have  $c$ -axis orientation.

From the optical images in Fig. 4 (c) to Fig. 4 (f), GdYBCO (c), (d) has many different colored grain (black, white, orange) and grain sizes are bigger than other samples. In this sample, overall Raman spectra in range of  $100\text{ cm}^{-1}$

to  $700\text{ cm}^{-1}$  was similar but higher frequency after  $700\text{ cm}^{-1}$  shows dependence on the grain the data are taken. Some black colored grain has intense oxygen peak in  $240\text{ cm}^{-1}$  and  $500\text{ cm}^{-1}$  to  $630\text{ cm}^{-1}$  (Fig. 4 (a)). Also more of second phase of CuO in  $294\text{ cm}^{-1}$  are observed in the black part . GdBCO (d), (f) has many different colored grains but size of the grains is much smaller than that of GdYBCO. Raman spectra of GdBCO is rather homogeneous with respect to the position but some white spot does not show the apical O(4) mode and O(2)+O(3) mode (Fig. 4 (b)). From these result, we can conclude that the black part contain more oxygen and in the case of GdYBCO, it contains more second phase of CuO than the white part.

Polarized Raman measurement can provide information regarding the structure of a sample.  $MBa_2Cu_3O_{7-x}$  is  $P_{mmm}$  space group and it can be grown either into orthorhombic or tetragonal structure and we can calculate the Raman activity of particular vibration modes that depends on the polarization configuration by using Raman tensor (Table 1 (a)). There are four Raman active  $A_g$ ,  $B_{1g}$ ,  $B_{2g}$ , and  $B_{3g}$  modes in the orthorhombic structure, and five modes of  $A_{1g}$ ,  $A_{2g}$ ,  $B_{1g}$ ,  $B_{2g}$ , and  $E_g$  are Raman active mode in the tetragonal structure of MBCO. Raman tensors of these modes are shown below [24].

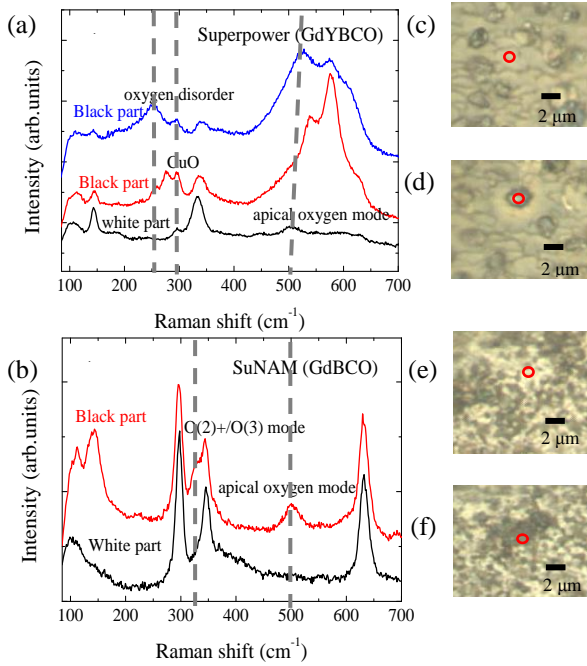


Fig. 4. Unpolarized Raman spectra of GdYBCO (a) and GdBCO (b) taken at different locations on the sample. Dashed lines in (a) represent the oxygen disorder ( $240\text{ cm}^{-1}$ ), the second phase of CuO ( $294\text{ cm}^{-1}$ ), and the apical oxygen ( $A_g$ ) mode (around  $500\text{ cm}^{-1}$ ) frequencies. Dashed lines in (b) is the O(2)+O(3) mode (around  $330\text{ cm}^{-1}$ ) and the apical oxygen ( $A_g$ ) mode (around  $500\text{ cm}^{-1}$ ). (c) and (e) are white part of the sample (denoted by a red circle) and (d) and (f) are black part of the sample (denoted by a red circle).

TABLE 1

RAMAN ACTIVE MODE OF EACH POLARIZATION CALCULATED BY RAMAN TENSOR OF SPACE GROUP  $P_{mmm}$  (A). IDENTIFYING THE STRUCTURE OF YBCO (B), GdYBCO (C) AND GdBCO (D) BY RELATIVE INTENSITY OF EACH POLARIZATION. S IS STRONG INTENSITY, W IS WEAK INTENSITY

	orthorhombic		Tetragonal			
XX	$A_g$		XX	$A_{1g}, B_{1g}$		
XY	$B_{1g}$		XY	$B_{2g}$		
X'X'			X'X'	$A_{1g}, B_{2g}$		
X'Y'	$A_g, B_{1g}$		X'Y'	$B_{1g}$		
YBCO Peak position( $\text{cm}^{-1}$ )						
Peak	210	140	333	448	494	
XX	S	S	S	W	W	
XY	S	W	W			
X'X'	S	S	W	W	W	
X'Y'	W	W	S			
Ortho		$A_g$	$A_g$	$A_g$	$A_g$	
Tetra	$A_{1g}, B_{2g}$	$A_{1g}$	$B_{1g}$	$A_{1g}$	$A_{1g}$	
GdYBCO Peakposition( $\text{cm}^{-1}$ )						
Peak	143	294	335	500	630	
XX	S	W	S	W		
XY	W	W	W	W	W	
X'X'	S	W	W	W	W	
X'Y'	W	W	W	W		
Ortho	$A_g$		$A_g$	$A_g$	$B_{1g}$	
Tetra	$A_{1g}$	$A_{1g}, B_{2g}$	$A_{1g}, B_{1g}$	$A_{1g}$	$B_{2g}$	
GdBCO Peakposition( $\text{cm}^{-1}$ )						
Peak	143	295	326	344	502	631
XX	S	S	S	S	S	W
XY	S	W	W	S	W	S
X'X'	S	S	W	W	W	W
X'Y'	W	W	S	W	W	W
Ortho	$A_g$	$A_g$	$A_g$	$A_g, B_{1g}$	$A_g$	$B_{1g}$
Tetra	$A_{1g}$	$B_{1g}$			$A_{1g}$	$B_{2g}$

$$\mathbf{A}_g = \begin{pmatrix} a & 0 & 0 \\ 0 & b & 0 \\ 0 & 0 & c \end{pmatrix} \quad \mathbf{B}_{1g} = \begin{pmatrix} 0 & d & 0 \\ e & 0 & 0 \\ 0 & 0 & 0 \end{pmatrix}$$

$$\mathbf{B}_{2g} = \begin{pmatrix} 0 & 0 & 0 \\ 0 & 0 & f \\ 0 & g & 0 \end{pmatrix} \quad \mathbf{B}_{3g} = \begin{pmatrix} 0 & 0 & 0 \\ 0 & 0 & h \\ 0 & i & 0 \end{pmatrix}$$

These are Raman tensor in the orthorhombic structure. We can calculate the Raman activity in a particular polarization configuration by multiplying the polarization state of light into the Raman tensors. Then, we can figure out the  $A_g$  mode is to be observed in  $XX$ ,  $X'X'$  and  $X'Y'$  polarization configurations and the  $B_{1g}$  mode is to be seen in  $X'X'$  and  $X'Y'$  polarization configurations.  $B_{2g}$  and  $B_{3g}$  modes cannot be observed in the  $c$ -axis orientation.

$$\mathbf{A}_{1g} = \begin{pmatrix} a & 0 & 0 \\ 0 & a & 0 \\ 0 & 0 & a \end{pmatrix} \quad \mathbf{A}_{2g} = \begin{pmatrix} 0 & c & 0 \\ -c & 0 & 0 \\ 0 & 0 & 0 \end{pmatrix}$$

$$\mathbf{B}_{1g} = \begin{pmatrix} d & 0 & 0 \\ 0 & -d & 0 \\ 0 & 0 & 0 \end{pmatrix} \quad \mathbf{B}_{2g} = \begin{pmatrix} 0 & e & 0 \\ e & 0 & 0 \\ 0 & 0 & 0 \end{pmatrix}$$

$$\mathbf{E}_g = \begin{pmatrix} 0 & 0 & f \\ 0 & 0 & 0 \\ g & 0 & 0 \end{pmatrix} \quad \text{or} \quad \begin{pmatrix} 0 & 0 & 0 \\ 0 & 0 & f \\ 0 & g & 0 \end{pmatrix}$$

These are Raman tensor in the tetragonal structure. By following the same procedure as with the orthorhombic structure, we can figure out the  $A_{1g}$  mode is to be observed in  $XX$  and  $X'X'$  polarization configuration, the  $B_{1g}$  mode is to be observed in  $XX$  and  $X'Y'$  polarization configuration, and the  $B_{2g}$  mode is to be seen in  $XY$  and  $X'X'$  polarization configuration.  $A_{2g}$  and  $E_g$  modes cannot be observed in the  $c$ -axis orientation. From these result, we could confirm that this samples are  $c$ -axis oriented

Fig. 5 plot polarized Raman spectra of the three samples. Table 1 shows the relative peak intensity of the three samples. From relative peak intensity of four polarization configurations, we can assign the Raman modes of each possible structure. In reference, all Raman modes of YBCO are  $A_g$  mode, especially  $O(2)+O(3)$  mode and apical  $O(4)$  modes are  $A_g$  mode. According to our result of the polarization dependence of  $A_g$  modes, it is confirmed that the three samples have orthorhombic structure.

#### 4. CONCLUSION

To study the local structure of MBCO coated conductor, we used polarized Raman spectroscopy. As contents change from Y to Gd, the  $O(2)+O(3)$  mode near  $330 \text{ cm}^{-1}$  red shifts. The apical  $O(4)$  mode near  $500 \text{ cm}^{-1}$  exhibits higher intensity in the black part of the optical image, which suggests that the black part contains more oxygen. Existence of the  $O(2)+O(3)$  mode can show that these samples are  $c$ -axis oriented. Calculating Raman activity of the  $A_g$  mode of  $O(2)+O(3)$  mode and apical  $O(4)$  modes

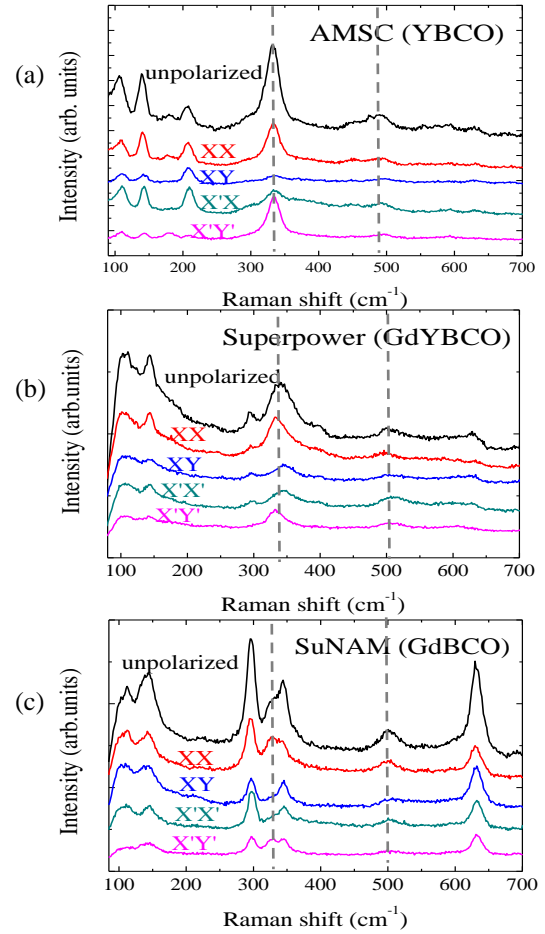


Fig. 5. Polarized Raman spectra of YBCO (a), GdYBCO (b) and GdBCO (c).  $X'$  and  $Y'$  are  $45^\circ$  tilted polarizations of  $X$  and  $Y$  polarization, respectively. Dashed lines are main peak of MBCO ( $A_g$  mode of  $330 \text{ cm}^{-1}$  and  $500 \text{ cm}^{-1}$ ).

with respect to the polarization configuration by using Raman tensor and comparing to parallel ( $XX$  and  $X'X'$ ) and two cross ( $XY$  and  $X'Y'$ ) polarization Raman measurements confirm that the three samples we studied have orthorhombic structure. Our results suggest that polarized Raman scattering spectroscopy can be effectively used as a local probe that can provide information regarding orientation and crystalline structure as well as the distribution of the secondary phase in micrometer scale.

#### ACKNOWLEDGMENT

This work was supported by the National Research Foundation of Korea (NRF) with grants funded by the Korea government (MSIP) (2013 R1A1A2007951 and 2014R1A2A2A01004070) and by the Korea Electrotechnology Research Institute (KERI) primary research program through the National Research Council of Science & Technology (NST) funded by the Ministry of Science, ICT and Future Planning (MSIP) (No. 15-12-N0101-34)

## REFERENCES

- [1] J. G. Bednorz, K. A. Müller, "Possible high  $T_c$  superconductivity in the Ba-La-Cu-O system," *Zeitschrift für Physik B*, vol. 64, pp. 189-193, 1986.
- [2] P. J. Ford, "The Rise of the Superconductors," *CRC Press*, 2005.
- [3] A. Schilling, M. Cantoni, J. D. Guo, H. R. Ott, "Superconductivity above 130 K in the Hg-Ba-Ca-Cu-O system," *Nature*, vol. 363, pp. 56-58, 1993.
- [4] N. Khare, "Handbook of High-Temperature Superconductor Electronics," *CRC Press*, 2003.
- [5] Y. Shiohara, T. Taneda, M. Yoshizumi, "Overview of Materials and Power Applications of Coated Conductors Project," *Jpn. J. Appl. Phys.*, vol. 51, pp. 010007(16pp), 2012.
- [6] N. Dechous, C. Jiménez, P. Chaudouët, L. Rapenne, E. Sarigiannidou, F. Robaut, S. Petit, S. Garaudée, L. Porcar, J. L. Soubeyrou, P. Odier, C. E. Bruzek, M. Decroux, "Textured YBCO films grown on wires: application to superconducting cables," *Supercond. Sci. Technol.*, vol. 25, pp. 125008(7pp), 2012.
- [7] X. Obradors, T. Puig, "Coated conductors for power applications: materials challenges," *Supercond. Sci. Technol.*, vol. 27, pp. 044003(17pp), 2014.
- [8] T. Aytug, M. Paranthaman, L. Heatherly, Y. Zuev, Y. Zhang, K. Kim, A. Goyal, V. A. Maroni, Y. Chen, V. Selvamanickam, "Deposition studies and coordinated characterization of MOCVD YBCO films on IBAD-MgO templates," *Supercond. Sci. Technol.*, vol. 22, pp. 015008(5pp), 2009.
- [9] W. Li, G. Li, B. Zhang, P. Chou, S. Liu, X. Ma, "Fabrication of GdBa<sub>2</sub>Cu<sub>3</sub>O<sub>7-δ</sub> films by photo-assisted-MOCVD process," *Physica C*, vol. 501, pp. 1-6, 2014.
- [10] X. Li, M. W. Rupich, T. Kodankandath, Y. Huang, W. Zhang, E. Siegal, D. T. Verebelyi, U. Schoop, N. Nguyen, C. Thieme, Z. Chen, D. M. Feldman, D. C. Lasbalestier, T. G. Holesinger, L. Civale, Q. X. Jia, V. Maroni, M. V. Rane, "High Critical Current YBCO Films Prepared by an MOD Process on RABiTS Templates," *IEEE Trans. Appl. Supercond.*, vol. 17, pp. 3553-3556, 2007.
- [11] T. Izumi, M. Yoshizumi, J. Nakaoka, Y. Kitoh, Y. Sutoh, T. Nakanishi, A. Nakai, K. Suzuki, Y. Yamada, A. Yajima, T. Saitoh, Y. Shiohara, "Progress in development of advanced TFA-MOD process for coated conductors," *Physica C*, vol. 463-465, pp. 510-514, 2007.
- [12] S. S. Oh, H. S. Ha, H. S. Kim, R. K. Ko, K. J. Song, D. W. Ha, T. H. Kim, N. J. Lee, D. Youm, J. S. Yang, H. K. Kim, K. K. Yu, S. H. Moon, K. P. Ko, S. I. Yoo, "Development of long-length SmBCO coated conductors using a batch-type reactive co-evaporation method," *Supercond. Sci. Technol.*, vol. 21, pp. 034003(6pp), 2008.
- [13] H. S. Kim, H. S. Ha, T. H. Kim, J. S. Yang, R. K. Ko, K. J. Song, D. W. Ha, N. J. Lee, S. S. Oh, D. J. Youm, C. Park, "The deposition of Sm<sub>1</sub>Ba<sub>2</sub>Cu<sub>3</sub>O<sub>7-δ</sub> on SrTiO<sub>3</sub> using co-evaporation method," *Physica C*, vol. 460-462, pp. 1361-1362, 2007.
- [14] M. P. Paranthaman, X. Qiu, F. A. List, K. Kim, Y. Zhang, X. Li, S. Sathyamurthy, C. Thieme, M. W. Rupich, "Development of Solution Buffer Layers for RABiTS Based YBCO Coated Conductors," *IEEE Trans. Appl. Supercond.*, vol. 21, pp. 3059-3061, 2011.
- [15] X. Xiong, S. Kim, K. Zdun, S. Sambandam, A. Rar, K. P. Lenseith, V. Selvamanickam, "Progress in High Throughput Processing of Long-Length, High Quality, and Low Cost IBAD MgO Buffer Tapes at SuperPower," *IEEE Trans. Appl. Supercond.*, vol. 19, pp. 3319-3322, 2009.
- [16] K. P. Ko, H. S. Ha, H. K. Kim, K. K. Yu, R. K. Ko, S. H. Moon, S. S. Oh, C. Park, S. I. Yoo, "Fabrication of highly textured IBAD-MgO template by continuous reel-to-reel process and its characterization," *Physica C*, vol. 463-465, pp. 564-567, 2007.
- [17] M. W. Rupich, X. Li, S. Sathyamurthy, C. L. H. Thieme, K. DeMoranville, J. Gannon, S. Fleshler, "Second Generation Wire Development at AMSC," *IEEE Trans. Appl. Supercond.*, vol. 23, pp. 6601205, 2013.
- [18] V. Selvamanickam, Y. Chen, X. Xiong, Y. Y. Xie, J. L. Reeves, X. Zhang, Y. Qiao, K. P. Lenseith, R. M. Schmidt, A. Rar, D. W. Hazelton, K. Tekletsadik, "Recent Progress in Second-Generation HTS Conductor Scale-Up at SuperPower," *IEEE Trans. Appl. Supercond.*, vol. 17, pp. 3231-3234, 2007.
- [19] J. H. Lee, H. J. Lee, S. M. Choi, S. I. Yoo, S. H. Moon, "RCE-DR, a novel process for coated conductor fabrication with high performance," *Supercond. Sci. Technol.*, vol. 27, pp. 044018(6pp), 2014.
- [20] M. F. Limonov, A. I. Rykov, S. Tajima, A. Yamanaka, "Raman scattering in YBa<sub>2</sub>Cu<sub>3</sub>O<sub>7</sub> single crystals: Anisotropy in normal and superconductivity states," *Physics of the Solid States*, vol. 40, pp. 367-376, 1998.
- [21] Z. Xhen, V. A. Maroni, D. J. Miller, X. Li, M. W. Rupich, R. Feenstra, "Examination of through-thickness/through-time phase evolution during an MOD-type REBCO precursor conversion using Raman microscopy," *Supercond. Sci. Technol.*, vol. 23, pp. 085006(9pp), 2010.
- [22] G. Kim, A.R. Jeong, W. Joa, D.Y. Park, H. Cheong, G.M. Shin, S.I. Yoo, "Optimal growth conditions for GdBa<sub>2</sub>Cu<sub>3</sub>O<sub>7</sub> thin-film coated conductors characterized by polarized Raman scattering spectroscopy," *Physica C*, vol. 470, pp. 1021-1024, 2010.
- [23] A. Fainstein, P. Etchegoin, J. Guimpel, "Raman study of photoinduced chain-fragment ordering in GdBa<sub>2</sub>Cu<sub>3</sub>O<sub>x</sub> thin films," *Phys. Rev. B*, vol. 58, pp. 9433-9439, 1998.
- [24] W. Hayes, R. Loudon, *Scattering of light by crystals*, A Wiley-Interscience publication, 1978.